Available online at www.sciencedirect.com
ScienceDirect
Ceramics International 37 (2011) 3781–3784
CERAMICS INTERNATIONAL
www.elsevier.com/locate/ceramint

Short communication

# Novel pulse ageing characteristics of ZPCCE varistor ceramics

Choon-W. Nahm *

*Semiconductor Ceramics Laboratory, Department of Electrical Engineering, Dongeui University, Busan 614-714, Republic of Korea*

Received 10 May 2011; received in revised form 9 June 2011; accepted 9 June 2011
Available online 15 June 2011

**Abstract**

The pulse ageing characteristics of the ZnO–$Pr_6O_{11}$–CoO–$Cr_2O_3$–$Er_2O_3$ varistor ceramics has been investigated for 0.5 and 2.0 mol% $Er_2O_3$. The breakdown field ($E_{1\ mA/cm^2}$) increased to almost double when $Er_2O_3$ increased from 0.5 to 2.0 mol%. The amount of $Er_2O_3$ addition did have a significant effect on clamp ratio, which exhibits a surge protection capability. The varistor ceramics added with 2.0 mol% exhibited the best clamp characteristics, in which the clamp voltage ratio was in the range of $K$ = 1.59–1.84 at a pulse-current of 5–50 A. The varistor ceramics added with 0.5 mol% $Er_2O_3$ exhibited excellent electrical stability, where $\%\Delta E_{1\ mA/cm^2} = -3.6\%$ and $\%\Delta\alpha = -10.0\%$ for the pulse-current of 2100 A.


*Keywords:* E. Varistors; Ceramics; Electrical measurement; Pulse-current; Ageing behavior

## 1. Introduction

Electrical overvoltages can cause either permanent deterioration, or temporary malfunctions in electronic components and systems. Protection from transients can be obtained by using specially designed components which will, either limit the magnitude of the transient using large series impedance or by diverting the transient using a low value shunt impedance.

ZnO varistors are switching devices, which depend on the applied voltage from their highly insulating state to highly conducting state. They act as an off state due to the high impedance at a low voltage and on state due to the low impedance at a high voltage. This shows highly nonlinear properties in the voltage–current relation. Based on the high nonlinearity, the varistors are widely used in the field of overvoltage protection systems from electronic circuits to electric power systems [1,2]. The structure of the body consists of a matrix of conductive zinc oxide grains separated by grain boundaries, which provide *p–n* junction semiconductor characteristics. The basic conduction mechanism of the varistors results from semiconductor junctions at the grain boundaries of zinc oxide grains. The varistors are a multi-junction device with a number of grains acting as a series-parallel combination between the electrical terminals.

Most investigations for ZnO–$Pr_6O_{11}$-based varistors have been reported on the microstructure and electrical properties in terms of additives and sintering process [3–12]. In particular, Nahm et al. reported the effect of rare earth oxides on electrical properties and its stability against the DC accelerated degradation stress [6–12].

Many Researchers are looking for novel varistors having a high nonlinearity and strong pulse ageing characteristics. A study on the effect of the additives on the clamping characteristics and electrical behavior of varistor properties against the surge with a high energy has been reported [12–15]. This paper reports that ZnO–$Pr_6O_{11}$–CoO–$Cr_2O_3$–$Er_2O_3$ (ZPCCE) varistor ceramics provide excellent pulse ageing characteristics.

## 2. Experimental procedure

Reagent-grade raw materials were used in proportions of (98.0–$x$) mol% ZnO + 0.5 mol% $Pr_6O_{11}$ + 1.0 mol% CoO + 0.5 mol% $Cr_2O_3$ + $x$ mol% $Er_2O_3$ ($x$ = 0.5 and 2.0). Raw materials were mixed by ball milling with zirconia balls and acetone in a polypropylene bottle for 24 h. The mixture calcined at 750 °C for 2 h was uniaxially pressed into discs of 10 mm in diameter and 1.5 mm in thickness at a pressure of 80 MPa. The discs were sintered for 2 h at 1345 °C. The sintered samples were lapped and polished to 1.0 mm thickness. The final samples were about 8 mm in diameter and 1.0 mm in thickness. Silver paste was coated on both faces

* Tel.: +82 51 890 1669; fax: +82 51 890 1664.
*E-mail address:* cwnahm@deu.ac.kr.

0272-8842/$36.00 
doi:10.1016/j.ceramint.2011.06.015

of the samples and the electrodes were formed by heating it at 600 °C for 10 min. The electrodes were 5 mm in diameter. The surface microstructure was examined by a scanning electron microscope (SEM, Hitachi S2400, Japan). The average grain size (d) was determined by the lineal intercept method, given by $d = 1.56L/MN$, where $L$ is the random line length on the micrograph, $M$ is the magnification of the micrograph, and $N$ is the number of the grain boundaries intercepted by the lines [16]. The sintered density ($\rho$) was measured by the Archimedes method.

The electric field–current density ($E$–$J$) characteristics were measured using a $V$–$I$ source (Keithley 237). The breakdown field ($E_{1\ \mathrm{mA/cm^2}}$) was measured at 1.0 mA/cm$^2$. In addition, the nonlinear coefficient ($\alpha$) is defined by the empirical law, $J = CE^{\alpha}$, where $J$ is the current density, $E$ is the applied electric field, and $C$ is a constant. $\alpha$ was determined in the current density range of 1.0–10 mA/cm$^2$, where $\alpha = (\log J_2 - \log J_1)/(\log E_2 - \log E_1)$, and $E_1$ and $E_2$ are the electric fields corresponding to $J_1 = 1.0$ mA/cm$^2$ and $J_2 = 10$ mA/cm$^2$, respectively.

The clamping voltage ($V_c$) was measured at a pulse current of 5 A, 10 A, 25 A, and 50 A using a surge generator (Tae-yang Eng. Kor) and oscilloscope (TeK 3020B). The pulse-current waveform had a width of 20 μs and a rise time of 8 μs. The clamp voltage ratio ($K = V_c/V_{\mathrm{mA}}$) is defined by the ratio of clamping voltage ($V_c$) to varistor voltage ($V_{1\ \mathrm{mA}}$) measured at 1.0 mA DC. The pulse ageing test was performed at 400, 900, 1200, 1500, 1800, and 2100 A using a surge generator. The time interval between each pulse-current cycle was 10 min. After applying the respective pulse-current, the $V$–$I$ characteristics were measured at room temperature.

## 3. Results and discussion

Fig. 1 shows SEM micrographs for different amounts of $Er_2O_3$. There is no remarkable difference in the phases, which consisted of ZnO grain and intergranular layer [8]. The average grain sizes were 14.1 μm and 8.5 μm, respectively, for 0.5 and 2.0 mol% $Er_2O_3$. Fig. 2 shows that XRD analysis reveals the presence of Pr-rich and Er-rich intergranular layer as a minor secondary phase, in addition to a major phase of hexagonal ZnO [8]. The more distribution of secondary phases may have a significant effect on pulse ageing behavior. The sintered densities were 5.59 g/cm$^3$ and 5.56 g/cm$^3$, respectively, for 0.5 and 2.0 mol% $Er_2O_3$. Therefore, the amount of $Er_2O_3$ in this composition and sintering process did not significantly modify the densification process [8].

The $E$–$J$ characteristics for different amounts of $Er_2O_3$ are designated as initial in Fig. 3. The $E$–$J$ characteristic parameters are summarized as an initial value in Table 1. The conduction characteristics of varistors are divided into prebreakdown region (a linear region with much higher impedance) and breakdown region (a nonlinear region with much lower impedance). The breakdown field ($E_{1\ \mathrm{mA}}$) increased significantly in a wide range from 1511 to 2981 V/cm with increasing amount of $Er_2O_3$. This is attributed to the increase in the number of grain boundaries caused by the decrease in the ZnO grain size. On the other hand, the nonlinear coefficient (α) increased from 40 to 47 with increasing amount of $Er_2O_3$.

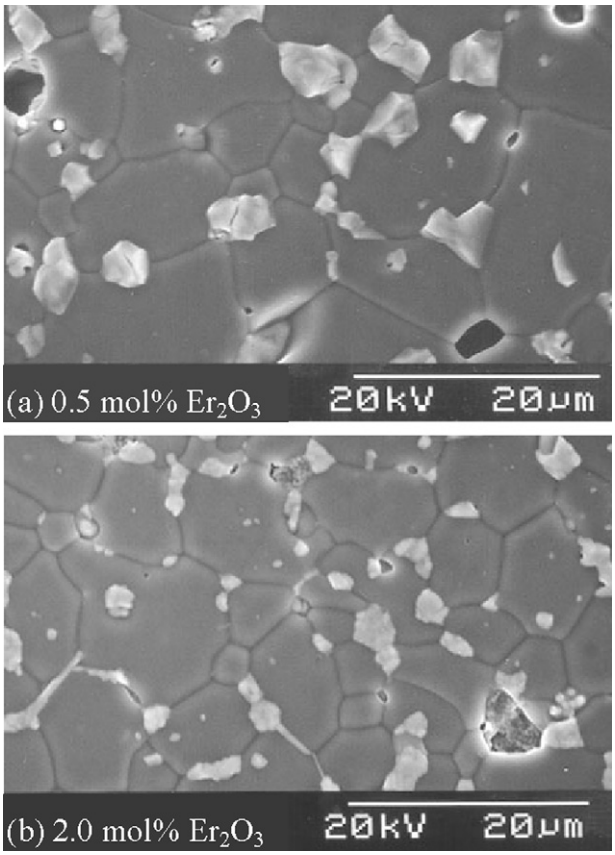


Fig. 1. SEM micrographs of the samples for different amounts of $Er_2O_3$.

Fig. 3 shows the clamping voltage ($V_c$) characteristics corresponding to a pulse-current of 1800 A for different amounts of $Er_2O_3$. The $V_c$ is defined by the drop voltage between the electrodes of the sample when the specified pulse-current flows through the sample. The higher pulse-current leads to the higher $V_c$ because the resistance in the nonlinear region exists still as a low value. It can be seen that the higher breakdown voltage leads to the higher clamping voltage. The $K$ at a pulse-current of 5–50 A was 1.68–2.0 for 0.5 mol% $Er_2O_3$

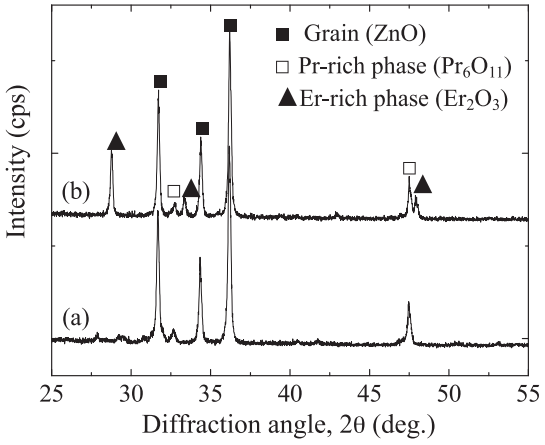


Fig. 2. XRD patterns of the samples for different amounts of $Er_2O_3$: (a) 0.5 mol% and (b) 2.0 mol%.

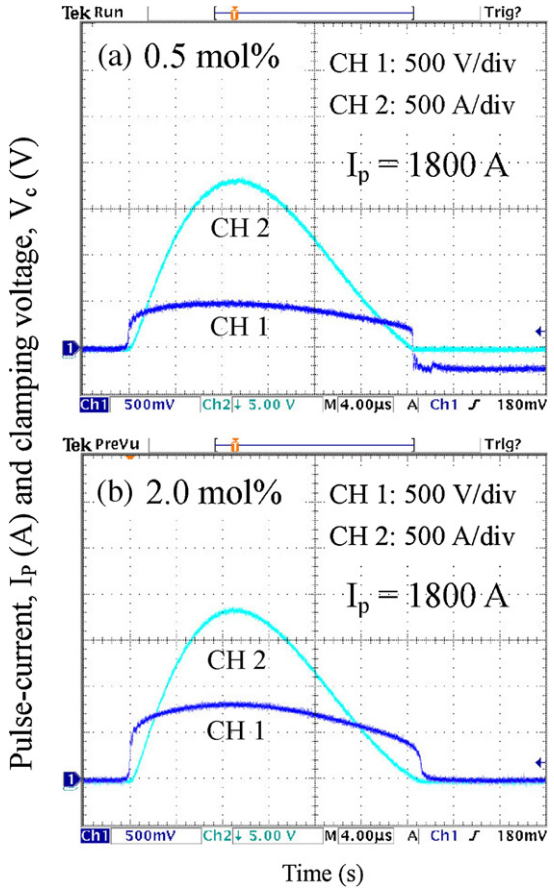


Fig. 3. Clamping voltage waveforms for a pulse-current of 1800 A of the samples for different amounts of $Er_2O_3$.

and 1.59–1.84 for 2.0 mol% $Er_2O_3$. The low $K$ value means that the varistor effectively clamps a pulse-current to the operating voltage. Based on the $\alpha$ and $K$ value in Table 1, it can be seen that a higher $\alpha$ value leads to a lower $K$ value. In order to obtain a low $K$ value, the $\alpha$ measured in the range of 1.0 mA/cm$^2$ and 10 mA/cm$^2$ have to be maintained it up to the high current region. In the light of the data shown in Table 1, it can be seen that the sample added with 2.0 mol% $Er_2O_3$ shows the best clamping characteristics for a pulse-current.

Fig. 4 compares the variation of $E$–$J$ characteristics after applying the pulse-current of 400–2100 A with the initial $E$–$J$ characteristics for the each sample. It should be noted that the pulse-current of 2100 A is very high pulse-current, compared with the size of sample. It can be seen that the $E$–$J$ characteristic curve shifted toward a low field region (downward in Fig. 4) in the breakdown region after applying the pulse-current stress. This is entirely different with the $E$–$J$ characteristic behavior, which shifted toward a high current region (rightward) in the prebreakdown region after applying the DC accelerated degradation stress [10]. The sample added with 0.5 mol% $Er_2O_3$ exhibited the smallest variation of the $>E$–$J$ characteristics in the nonlinear region. On the contrary, the sample added with 2.0 mol% $Er_2O_3$ exhibited the largest variation in the nonlinear region. The detailed electrical parameters after applying the pulse-current are summarized in Table 1. The sample added with 0.5 mol% $Er_2O_3$ exhibited very small $\%\Delta E_{1\ \mathrm{mA/cm^2}}$ less than 1% after applying the pulse-current stress less than 1500 A. Furthermore, the $\%\Delta E_{1\ \mathrm{mA/cm^2}}$ of this sample after applying the pulse-current of 2100 A was only −3.6%. The $\%\Delta E_{1\ \mathrm{mA/cm^2}}$ after applying the pulse current of 400 A for electrode size of 5 mm in commercial varistors is specified as the variation rate less than 10%. Therefore, it can be seen that how excellent this sample really is. While, the sample added with 2.0 mol% $Er_2O_3$ exhibited −3.9% for

Table 1
Breakdown field ($E_{1\ \mathrm{mA/cm^2}}$), nonlinear coefficient ($\alpha$), varistor voltage ($V_{1\ \mathrm{mA}}$), clamping voltage ($V_c$), clamp voltage ratio ($K$), variation of breakdown field ($\%\Delta E_{1\ \mathrm{mA/cm^2}}$), and variation of nonlinear coefficient ($\%\Delta\alpha$) of the samples after applying the pulse-current with different amounts of $Er_2O_3$.

| $Er_2O_3$ amount (mol%) | $E_{1\ \mathrm{mA/cm^2}}$ (V/cm) | $\alpha$ | $V_{1\ \mathrm{mA}}$ (V/mm) | $V_c$ (V) | | | | $K = V_c/V_{\mathrm{mA}}$ | | | |
|---|---|---|---|---|---|---|---|---|---|---|---|
| | | | | $I_p$ (A) = 5 A | 10 | 25 | 50 | $I_p$ = 5 A | 10 | 25 | 50 |
| 0.5 | 1511 | 40 | 157 | 264 | 272 | 294 | 314 | 1.68 | 1.73 | 1.87 | 2.0 |
| 2.0 | 2981 | 47 | 309 | 490 | 514 | 540 | 568 | 1.59 | 1.66 | 1.75 | 1.84 |

| | Pulse-current (A) | $E_{1\ \mathrm{mA/cm^2}}$(V/cm) | $\%\Delta E_{1\ \mathrm{mA/cm^2}}$ | $\alpha$ | $\%\Delta\alpha$ |
|---|---|---|---|---|---|
| 0.5 | Initial | 1511 | – | 40 | 0 |
| | 400 | 1509 | −0.1 | 40 | 0 |
| | 900 | 1506 | −0.3 | 40 | 0 |
| | 1200 | 1502 | −0.6 | 40 | 0 |
| | 1500 | 1500 | −0.7 | 39 | −2.5 |
| | 1800 | 1479 | −2.1 | 38 | −5 |
| | 2100 | 1457 | −3.6 | 36 | −10 |
| 2.0 | Initial | 2981 | – | 47 | – |
| | 400 | 2932 | −1.6 | 48 | 2.1 |
| | 900 | 2863 | −3.9 | 45 | −4.2 |
| | 1200 | 2476 | −16.9 | 31 | −34.0 |
| | 1500 | 2154 | −27.7 | 30 | −36.2 |
| | 1800 | 1391 | −53.3 | 19 | −59.6 |
| | 2100 | Failure | | | |

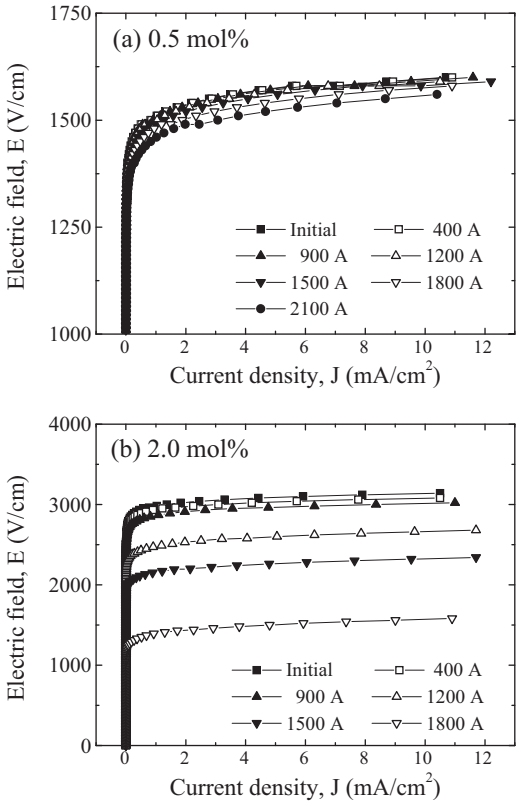


Fig. 4. *E–J* characteristics of the samples before and after applying the pulse-current with different amounts of $Er_2O_3$.

$\%\Delta E_{1\ mA/cm^2}$ at the pulse-current of 900 A. The breakdown field of this sample decreased abruptly with increasing pulse-current strength. Eventually, this sample was destroyed at the pulse-current of 2100 A. The $\%\Delta\alpha$ after applying the pulse-current of 1800 A was −5.0% for the sample added with 0.5 mol% $Er_2O_3$, whereas −59.6% for the sample added with 2.0 mol% $Er_2O_3$. The sample with 2.0 mol% $Er_2O_3$ is comparatively low stability, compared with the sample with 0.5 mol% $Er_2O_3$. This is because the more secondary phases provide a limited current path against pulse-current due to the decreased effective grain boundary area. On the whole, the samples added with 0.5 mol% $Er_2O_3$ showed excellent varistor characteristics in terms of pulse ageing characteristics as well as high nonlinear properties.

## 4. Conclusions

The pulse ageing characteristics of the ZnO–$Pr_6O_{11}$–CoO–$Cr_2O_3$–$Er_2O_3$ varistor ceramics has been investigated for 0.5 and 2.0 mol% $Er_2O_3$. The breakdown field ($E_{1\ mA/cm^2}$) increased to almost double when $Er_2O_3$ increased from 0.5 to 2.0 mol%. The varistor ceramics added with 2.0 mol% exhibited the best clamp characteristics, in which the clamp voltage ratio was in the range of $K = 1.59$–$1.84$ at a pulse-current of 5–50 A. The varistor ceramics added with 0.5 mol% $Er_2O_3$ exhibited excellent electrical stability, where $\%\Delta E_{1\ mA/cm^2} = -3.6\%$ and $\%\Delta\alpha = -10.0\%$ for the pulse-current of 2100 A.

## References

[1] L.M. Levinson, H.R. Philipp, Zinc oxide varistor: a review, Am. Ceram. Soc. Bull. 65 (1986) 639–646.
[2] T.K. Gupta, Application of zinc oxide varistor, J. Am. Ceram. Soc. 73 (1990) 1817–1840.
[3] A.B. Alles, V.L. Burdick, The effect of liquid-phase sintering on the properties of $Pr_6O_{11}$-based ZnO varistors, J. Appl. Phys. 70 (1991) 6883–6890.
[4] A.B. Alles, R. Puskas, G. Callahan, V.L. Burdick, Compositional effects on the liquid-phase sintering of praseodymium oxides-based zinc oxides varistors, J. Am. Ceram. Soc. 76 (1993) 2098–2102.
[5] Y.-S. Lee, K.-S. Liao, T.-Y. Tseng, Microstructure and crystal phases of praseodymium in zinc oxides varistor ceramics, J. Am. Ceram. Soc. 79 (1996) 2379–2384.
[6] C.-W. Nahm, The nonlinear properties and stability of ZnO–$Pr_6O_{11}$–CoO–$Cr_2O_3$–$Er_2O_3$ ceramic varistors, Mater. Lett. 47 (2001) 182–187.
[7] C.-W. Nahm, B.-C. Shin, Highly stable electrical properties of ZnO–$Pr_6O_{11}$–CoO–$Cr_2O_3$–$Y_2O_3$-based varistor ceramics, Mater. Lett. 57 (2003) 1322–1326.
[8] C.-W. Nahm, Electrical properties and stability against DC accelerated aging stress of ZPCCE-based varistor ceramics, J. Mater. Sci.: Mater. Electron. 15 (2004) 29–36.
[9] C.-W. Nahm, Microstructure and electrical properties of $Dy_2O_3$-based ZnO–$Pr_6O_{11}$-based varistor ceramics, Mater. Lett. 58 (2004) 2252–2255.
[10] C.-W. Nahm, B.-C. Shin, Effect of sintering time on electrical characteristics and DC accelerated aging behaviors of Zn–Pr–Co–Cr–Dy oxide-based varistors, J. Mater. Sci.: Mater. Electron. 16 (2005) 725–732.
[11] C.-W. Nahm, Effect of sintering temperature on nonlinear electrical properties and stability against DC accelerated aging stress of (CoO, $Cr_2O_3$, $La_2O_3$)-doped ZnO–$Pr_6O_{11}$-based varistors, Mater. Lett. 60 (2006) 3311–3314.
[12] C.-W. Nahm, Electrical properties and stability of Tb-doped ZnO-based nonlinear resistors, Solid State Commun. 141 (2007) 685–690.
[13] C.-W. Nahm, Highly stable nonlinear behavior against impulse current of ZnO–$Pr_6O_{11}$–CoO–$Cr_2O_3$–$Y_2O_3$ varistors, Mater. Lett. 64 (2010) 2631–2634.
[14] C.-W. Nahm, Major effects on impulse aging behavior of ZnO–$Pr_6O_{11}$–CoO–$Cr_2O_3$–$Er_2O_3$ varistor ceramics with small sintering changes, J. Am. Ceram. Soc. 93 (2010) 3056–3059.
[15] C.-W. Nahm, Impulse aging behavior against of Zn–Pr–Co–Cr–Dy varistors with cobalt addition, J. Am. Ceram. Soc. 94 (2011) 328–331.
[16] J.C. Wurst, J.A. Nelson, Lineal intercept technique for measuring grain size in two-phase polycrystalline ceramics, J. Am. Ceram. Soc. 55 (1972) 109–111.